In Vivo ^{1}H NMR Spectroscopy of the Human Brain at High Magnetic Fields: Metabolite Quantification at 4T vs. 7T

Ivan Tkáč[*], **Gülin Öz**, **Gregor Adriany**, **Kamil Uğurbil**, and **Rolf Gruetter**
Center for Magnetic Resonance Research, University of Minnesota, Minneapolis, Minnesota, USA.

Abstract

A comprehensive comparative study of metabolite quantification from the human brain was performed on the same 10 subjects at 4T and 7T using MR scanners with identical consoles, the same type of RF coils, and identical pulse sequences and data analysis. Signal-to-noise ratio (SNR) was increased by a factor of 2 at 7T relative to 4T in a volume of interest selected in the occipital cortex using half-volume quadrature radio frequency (RF) coils. Spectral linewidth was increased by 50% at 7T, which resulted in a 14% increase in spectral resolution at 7T relative to 4T. Seventeen brain metabolites were reliably quantified at both field strengths. Metabolite quantification at 7T was less sensitive to reduced SNR than at 4T. The precision of metabolite quantification and detectability of weakly represented metabolites were substantially increased at 7T relative to 4T. Because of the increased spectral resolution at 7T, only one-half of the SNR of a 4T spectrum was required to obtain the same quantification precision. The Cramér-Rao lower bounds (CRLB), a measure of quantification precision, of several metabolites were lower at both field strengths than the intersubject variation in metabolite concentrations, which resulted in a strong correlation between metabolite concentrations of individual subjects measured at 4T and 7T.

Keywords

MRS; high field; quantification; LCModel; field comparison

The potential of high-field in vivo ^{1}H NMR spectroscopy to provide extended neurochemical information based on increased sensitivity and spectral resolution was demonstrated approximately a decade ago (1,2). Since then, a number of comparison studies have investigated the improvement in signal-to-noise ratio (SNR), spectral resolution, and the precision of metabolite quantification with an increase in static magnetic field B_0 (3-10). However, reported gains in SNR and metabolite quantification have not been consistent, which might be explained by the complexity of the comparison of two different MR scanners operating at different B_0 values. A number of factors influence the SNR, spectral resolution, and ultimately the quantification precision, such as functionality of the transmit and receive channels, B_0 shimming efficiency, radio frequency (RF) coils, pulse sequence design, and data processing (11). Increases in SNR by 20% to 46% at 3T relative to 1.5T were reported in single-voxel (3,7) and chemical-shift imaging (CSI) studies (5,6) of the human brain. Modest increase (5), almost no improvement (3), or even decrease (7) in spectral resolution (ppm) at 3T relative to 1.5T have been observed. The diagnostic accuracy of ^{1}H NMR spectroscopy to distinguish

*Correspondence to: Ivan Tkáč, Center for Magnetic Resonance Research, Department of Radiology, University of Minnesota, 2021 6th Street SE, Minneapolis, MN 55455. ivan@cmrr.umn.edu.
Current address for Rolf Gruetter: Laboratory of Functional and Metabolic Imaging, Ecole Polytechnique Federale de Lausanne, Lausanne, Switzerland.

patients with Alzheimer disease from cognitively normal subjects was not improved at 3T relative to 1.5T (7). On the other hand, precision and reproducibility of *myo*-inositol quantification were significantly increased in another comparative study at 3T vs. 1.5T (10). The SNR in human brain stimulated-echo acquisition mode (STEAM) spectra was increased by ~80% at 4T relative to 1.5T (4), while SNR of singlet resonances increased linearly with increasing B_0 using proton echo-planar spectroscopic imaging (PEPSI) at different field strengths between 1.5T and 7T (8). A significant increase in the reliability of quantification of metabolites with J-coupled spin systems was described at 4T relative to 1.5T (4) and 3T (9).

Increased availability of 7T whole-body MR scanners in recent years stimulates an interest in evaluating the pros and cons of in vivo ^{1}H NMR spectroscopy at ultrahigh magnetic fields. Several years ago we have demonstrated the feasibility of in vivo ^{1}H NMR spectroscopy of the human brain at 7T and reported substantial improvements in sensitivity and spectral resolution (12). Previous comparative studies were mainly focused on the field dependence of SNR (3,5,8). The purpose of the current study was a quantitative evaluation of gains in NMR spectroscopy at ultrahigh magnetic fields with the main emphasis on precision and accuracy of metabolite quantification. To achieve this goal, a comprehensive comparison study was performed at 4T and 7T. To separate the effect of increased B_0 as much as possible from other factors influencing sensitivity, spectral resolution, and metabolite quantification, the same 10 subjects were scanned both at 4T and 7T using identical consoles, similar design of RF coils, and identical pulse sequences and data processing.

MATERIALS AND METHODS

Subjects

Ten healthy volunteers (3 females, 7 males, age range = 24 ± 5 years) participating in this comparison study were examined both at 4T and 7T within 1 to 10 d. The study protocol was approved by the Institutional Review Board and all subjects provided informed written consent before study participation.

MR Scanners

The measurements were performed using 4T and 7T whole-body magnets interfaced to Varian INOVA consoles (Varian, Inc., Palo Alto, CA, USA). The 4T/90-cm magnet (Siemens/Oxford Magnet Technology, UK) was equipped with a gradient system (40 mT/m, 400 μs rise-time), which included second-order shim coils with maximum shim strengths of $XZ = YZ = 5$ Hz/cm^2, $Z2 = 12$ Hz/cm^2, and $XY = X2-Y2 = 2.5$ Hz/cm^2. The 7T/90-cm magnet (Magnex Scientific, UK) was equipped with a head gradient coil (40 mT/m, 500 μs rise-time) and strong second-order shim coils (Magnex Scientific) with maximum strengths of $XZ = YZ = 25$ Hz/cm^2, $Z2 = 38$ Hz/cm^2, and $XY = X2-Y2 = 12$ Hz/cm^2. Shim coil currents were controlled using amplifiers from Resonance Research, Inc. (Billerica, MA, USA). The RF amplifiers (CPC, Brentwood, NY, USA) provided maximum power of 2.6 kW (4T) and 4.5 kW (7T) at the coil. Half-volume RF coils of similar design (13) combined with quadrature hybrids with fixed 90° phase shift were used for RF signal transmission and reception at both field strengths. The two geometrically decoupled circular coil loops of the 4T RF coil were 14 cm in diameter. To adjust for the difference in RF field penetration at the higher frequency due to more complex B_1 fields, the loop shape of the 7T RF coil was slightly modified toward an elliptical loop design with dimensions along the short and long axes of 11 cm and 15 cm, respectively. The shorter axis of the 7T coil loops was along the Z-axis of the magnet. Using the aforementioned RF amplifiers and RF coils, the maximum transmit B_1^+ field was just above 40 μT in the center of the occipital lobe.

MRI

Transverse RARE (rapid acquisition with relaxation enhancement) images and sagittal TurboFLASH (turbo fast low-angle shot images) were used for the precise positioning of the volume of interest (VOI) in the occipital lobe of participating subjects. MR images from 4T studies were used to guide the VOI selection at 7T and vice-versa to guarantee that for each subject the same VOI in the brain was selected for spectroscopy at 4T and 7T. Parameters of RARE imaging were repetition time (TR)/echo time (TE)/echo spacing (ES) = 4000 ms/60 ms/ 15 ms at 4T and TR/TE/ES = 5000 ms/48 ms/12 ms at 7T, echo train length (ETL) = 8, number of transients (NT) = 2, slice thickness (THK) = 4 mm (at 4T) and THK = 2 mm (at 7T). Parameters for TurboFLASH imaging were inversion time (TI)/TR/TE = 1200 ms/11 ms/5 ms, and THK = 5 mm at 4T and TI/TR/TE = 1450 ms/12 ms/5 ms and THK = 4 mm at 7T, NT = 2. Specific absorption rates (SARs) were maintained within U.S. Food and Drug Administration (FDA) guidelines for all measurements.

^{1}H NMR Spectroscopy

All first- and second-order shim terms were automatically adjusted using FASTMAP (fast, automatic shimming technique by mapping along projections) with echo-planar imaging (EPI) readout (14,15). Ultrashort echo-time STEAM pulse sequence optimized for 4T (TR/TM/TE = 5000 ms/42 ms/4 ms) and 7T (TR/TM/TE = 5000 ms/32 ms/6 ms) was used for spectroscopic data acquisition (12,16). The spectral width (sw = 6 kHz) and the number of acquired complex points (np = 4096) were identical for both field strengths. The STEAM sequence was combined with outer volume suppression (OVS) to improve the localization performance. The water signal was efficiently suppressed by variable-power RF pulses with optimized relaxation delays (VAPOR) (16,17). STEAM 90° RF pulses were used for the local RF power adjustment and the power of all other pulses in OVS and VAPOR water suppression was automatically set. Data were acquired from 8-ml volumes (VOI = $2 \times 2 \times 2$ cm^3) centered on the midline in the occipital lobe. Data (free induction decay [FIDs]) were acquired in a "single-scan mode," which means that each single scan (transient) was saved separately. The total number of acquired transients was 160. In addition, un-suppressed water signal was acquired for eddy current correction (with OVS) and for metabolite quantification (without OVS).

Data Processing

Time domain frequency and phase correction were applied on single-scan data. Then a different number of single scan FIDs were chosen from the whole set of 160 FIDs and summed, creating 49 summed FIDs from each subject as follows: 10 FIDs with NT = 2, 10 × NT = 4, 10 × NT = 8, 10 × NT = 16, 5 × NT = 32, 2 × NT = 64, 1 × NT = 128, and 1 × NT = 160. This summing was repeated for all 10 subjects and both field strengths, creating 960 FIDs in total. All summed FIDs were corrected for residual eddy currents using unsuppressed signal of water acquired with OVS and finally an automatic zero-order phase correction was applied on data in time domain (subtraction of the phase of the first point of FID).

Metabolite Quantification

In vivo ^{1}H NMR spectra were analyzed using LCModel (18,19). The unsuppressed water signal measured from the same VOI without OVS was used as an internal reference for quantification, assuming 80% brain water content. LC-Model basis sets for 4T and 7T included spectra of 19 brain metabolites: alanine (Ala), ascorbate (Asc), aspartate (Asp), creatine (Cr), phosphocreatine (PCr), γ-aminobutyric acid (GABA), glucose (Glc), glutamate (Glu), glutamine (Gln), glutathione (GSH), glycerophosphorylcholine (GPC), phosphorylcholine (PCho), glycine, *myo*-inositol (*myo*-Ins), *scyllo*-inositol (*scyllo*-Ins), lactate (Lac), N-acetylaspartate (NAA), N-acetylaspartylglutamate (NAAG), phosphorylethanolamine (PE), and taurine (Tau). All spectra for both 4T and 7T basis sets were simulated using Varian

spectrometer spin-simulation software (neglecting J-evolution for ultrashort TE) based on a recently updated database of chemical shifts and coupling constants (20,21). Averaged spectra of fast relaxing macromolecules measured from five subjects at 4T and 7T using metabolite nulling inversion-recovery experiments with a short repetition time (TR = 2 s, TI = 0.675 s) were also included in the 4T and 7T LCModel basis sets. Before putting macromolecule spectra into the LCModel basis set, the residual signal of PCr with a short T_1 was removed from FIDs and the high-frequency noise was suppressed by the Gaussian filter (σ= 0.05 s). The LCModel analysis was performed on spectra within the chemical shift range 0.5–4.2 ppm. The default value of the LCModel parameter DESDSH, controlling the uncertainty in referencing between in vivo spectra and spectra in the LCModel basis set, was decreased from 0.004 ppm to 0.002 ppm. All four parameters controlling the zero- and first-order phase correction and their deviations were set to zero. The hidden parameter DKNTMN, controlling the knot spacing for the spline baseline fitting, was set to 0.20. LCModel analysis was performed in chemical shift range 0.5–4.2 ppm.

Cramér-Rao lower bounds (CRLB) of LCModel analysis were used to eliminate meaningless fitting results with extremely high estimated errors. Metabolites quantified with CRLB above 100% were excluded from further analysis. If a metabolite was not quantified with CRLB < 100% in at least 50% of analyzed spectra of a given subject and a given number of summed transients, then this metabolite was eliminated from further analysis for this subject and NT. If a metabolite was not quantified from spectra with a given NT for at least five subjects, then this metabolite was eliminated from further analysis. Finally, if the average CRLB of a specific metabolite was higher than 50%, this metabolite was considered "not detectable" under these conditions (B_0, NT). The correlation matrix from the detailed LCModel output was used to evaluate the correlation between fitted concentrations of metabolites with similar spectral patterns and high spectral overlap. t-Tests with and without corrections for multiple comparisons were used to evaluate the statistical significance of differences between 4T and 7T data. Average values are always reported as mean ± SD.

RESULTS

Ten healthy volunteers were scanned both at 4T and 7T and in vivo ^{1}H NMR spectra were acquired from the same location in the occipital lobe. Spectral quality achieved at 4T and 7T; the consistency in VOI selection on the two scanners is shown in Fig. 1. Highly efficient water suppression and elimination of signals from outside the VOI resulted in artifact-free spectra with a flat baseline without any residual water signal removal and baseline correction. Increased sensitivity at 7T is demonstrated by the ability to detect very weak signals, such as the H-1 signal of α-D-glucose at 5.22 ppm. This spectral quality was consistently achieved throughout the whole study, which is evident from Fig. 2, where spectra of all 10 subjects acquired at 4T and 7T are presented. FASTMAP shimming resulted in very reproducible spectral resolution, which can be seen from the characteristic multiplet patterns of glutamate at 2.35 ppm at 4T and of *myo*-inositol 3.6 ppm at 7T (Figs. 1 and 2). The water signal linewidth was 8.2 ± 0.6 Hz at 4T and 12.3 ± 1.1 Hz at 7T, corresponding to an increase at 7T by a factor of 1.50 ± 0.07 relative to 4T. In addition, a strong positive correlation ($R = 0.84$) was found between water signal linewidths of individual subjects at 4T and 7T (Fig. 3). Specifically, two subjects with the largest line-width at 4T had also the largest linewidth at 7T, and the same subject had the smallest linewidth at 4T and 7T (Fig. 3). Metabolite linewidths, determined from the singlet of total creatine at 3.03 ppm, were smaller than linewidths of corresponding water signals by 2.3 ± 0.6 Hz at 4T and by 2.5 ± 0.5 Hz at 7T.

SNRs were calculated from nonfiltered spectra using the maximum height of signal at the position of NAA methyl resonance at 2.008 ppm. Averaged SNR of spectra with NT = 160 was 102 ± 12 at 4T and 194 ± 27 at 7T, which corresponded to an increase in SNR at 7T by a

factor of 1.91 ± 0.13. The ratio of measured signal intensities (heights) at the position of NAA methyl resonance between 7T and 4T was 1.76 ± 0.13, and the ratio of noise levels between 7T and 4T was 0.92 ± 0.03. To also compare integral to noise ratios at two fields, the unsuppressed water signal was used. The ratio between integrals of water signals at 7T and 4T was 2.8 ± 0.2.

Concentrations of 16 metabolites and the content of fast relaxing macromolecules were quantified with CRLB < 50% from all in vivo ^{1}H NMR spectra (NT = 160) of 10 subjects measured at 4T and 7T (Fig. 4). In addition, *scyllo*-Ins was quantified from spectra of all subjects at 7T and of eight subjects at 4T. Quantification of the macromolecule content was highly reproducible with the coefficient of variation below 6%. Metabolite concentrations quantified at 4T and 7T were in excellent agreement; the average difference between concentrations obtained at 4T and 7T was only 0.16 μmol/g. Of all 17 metabolites and three combined pairs of metabolites (Fig. 4), only differences in concentrations of Asp, Cr, GABA, NAAG, and PE were significant ($P < 0.05$). When the Bonferroni correction for multiple comparisons was applied, only differences in Asp and GABA remained significant. Despite the significance level, differences in concentrations of these five metabolites obtained at 4T and 7T were very small, less than 0.6 μmol/g. Consistent quantification of Ala was possible only at 7T (0.16 ± 0.07 μmol/g, $N = 6$) and of Glc only at 4T (1.2 ± 0.5 μmol/g, $N = 10$); therefore these metabolites were omitted from the bar diagram in Fig. 4.

The mean SDs across all metabolites were nearly identical at 4T and 7T (0.32 μmol/g, error bars in Fig. 4) and substantially higher than the mean estimated error of metabolite quantification (mean CRLB) at 4T (0.20 μmol/g) and at 7T (0.11 μmol/g). This comparison indicated that the intersubject variation is the dominant source for the observed variance in metabolite levels. In fact, a strong positive correlation between concentrations obtained from 4T and 7T spectra was found for multiple brain metabolites (Fig. 5). In addition, clusters of points on scatter plots, representing measurements from individual subjects, were directly on the lines of identity. These data demonstrated the potential of ^{1}H NMR spectroscopy at 4T and 7T to quantify brain metabolites in absolute concentration units. A strong correlation between 4T and 7T data confirmed that the dominant source for variations in calculated concentrations were not errors of measurement, but real differences of metabolite levels in the brains of participating subjects. For example, two subjects with the lowest Gln concentration at 4T were the same two subjects with the lowest Gln at 7T; the highest level of Lac was found in the same subject at 4T and 7T; and similarly, the lowest level of Lac was found in another subject at both fields. Furthermore, the two subjects for whom *scyllo*-inositol was not quantified at 4T had the lowest *scyllo*-Ins concentrations at 7T, close to 0.10 μmol/g.

To investigate the effect of SNR on metabolite quantification, 4T and 7T spectra with different number of transients (NT = 2 to 128) were analyzed using LCModel (Fig. 6). As expected, estimated errors in quantification of metabolite concentrations (error bars in Fig. 6) increased with decreasing SNR (lower number of transients). When SNR dropped below a certain threshold, quantification of some weakly represented metabolites, such as GABA, NAAG, PE, or PC, was not possible at 4T. Decreased SNR resulted in systematic errors in quantification of metabolites, causing deviations of means from values determined from spectra with high SNR. This effect was more noticeable at 4T. At 7T, measured metabolite concentrations were nearly independent of NT, except for Asp, GABA, and PE.

CRLBs of LCModel analysis were used to evaluate the precision of metabolite quantification at 4T and 7T. Comparison of CRLBs as a function of the number of summed transients clearly demonstrated that for a given number of transients, estimated errors of quantification were always smaller at 7T than at 4T (Fig. 7). This could be expected, because 7T spectra had two times higher SNR than 4T spectra for a given number of transients. However, even when

comparing CRLB from spectra with the same SNR, e.g., spectra with NT =128 at 4T vs. spectra with NT = 32 at 7T, the precision of metabolite quantification was still better at 7T. The precision of metabolite quantification achieved at 4T for NT = 128 (dashed lines in Fig. 7) corresponded to the precision of quantification achieved at 7T for NT = 4 to 8. To verify the validity of this gain in quantification precision with increased field strength, LC-Model analysis of 4T spectra with NT = 128 was further compared to the analysis of 7T spectra with NT = 8, which had two-fold lower SNR than the 4T spectra (Fig. 8). Metabolite concentrations quantified at 4T (NT = 128) and 7T (NT = 8) were in very good agreement (Fig. 9). Only concentrations of Asp, Cr, and NAAG quantified at 4T and 7T were significantly different ($P < 0.05$); however, the difference was only 0.6 μmol/g on average. CRLBs at 7T (NT = 8) were similar or even slightly lower than those at 4T (NT = 128) (Fig. 9).

LCModel correlation coefficients between fitted metabolite concentrations were more negative than −0.5 for the following pairs of metabolites: Cr and PCr, PC and GPC, and PC + GPC and PE both at 4T and 7T; NAA and NAAG, and Glc and Tau at 4T. Comparison of LCModel correlation coefficients of selected pairs of metabolites between 4T and 7T is shown in Fig. 10a and b. The pair of glutamine and glutamate was also included (Fig. 10c) to demonstrate a very weak correlation between them even at low SNR. The magnitude of the LCModel correlation coefficients between NAA and NAAG were systematically lower at 7T. LCModel fitting anticipated a strong negative correlation between Cr and PCr in a broad range of SNR values for both 4T and 7T spectra (Fig. 10a). A similar dependence was observed for the pair PC and GPC, with the only difference that PC was not detectable in 4T spectra with low SNR (NT < 64). In order to evaluate to which extent LCModel correlation coefficients accurately predicted a correlation between assessed concentrations of these pairs of metabolites, their concentrations measured in 10 subjects were compared in scatter plots (Fig. 10d–i). A negative correlation ($R < −0.3$) was not found for any pair of metabolites from spectra of any number of transients.

DISCUSSION

The results of the present study clearly demonstrate advantages of ^{1}H NMR spectroscopy at ultrahigh magnetic fields for noninvasive metabolite quantification in the human brain. Increased sensitivity and spectral resolution at 7T relative to 4T substantially improved the precision of metabolite quantification and expanded the potential to detect and reliably quantify weakly represented metabolites. In general, fair field comparison is inherently prone to difficulties resulting from the fact that data has to be generated on two different MR scanners, which may perform considerably differently. In this study we minimized such differences by using 4T and 7T MR scanners with identical consoles and very similar design of RF coils, by using the same pulse sequence, same processing tools, and an LCModel basis set simulated from the same source of metabolite NMR data. In addition, data were collected from the same group of 10 subjects and an extra effort was made to select the same VOI at both field strengths.

An unbiased comparison of ^{1}H NMR spectroscopy at different fields requires spectra free of artifacts and distortions originating from an insufficient water suppression and insufficient suppression of signals from outside of the VOI, such as signals of subcutaneous lipids. In addition, macroscopic B_0 inhomogeneity in the VOI has to be minimized as much as possible in order to achieve the highest spectral resolution at the given field strength, limited by intrinsic properties of the studied tissue and T_2 relaxation. An ultrashort echo-time STEAM sequence optimized for 4T and 7T provided very reproducible and clean spectra (Figs. 1 and 2). FASTMAP shimming and sufficiently strong second-order shim systems were essential for suppressing macroscopic B_0 inhomogeneity in the measured VOI to a negligible level and enabled to achieve high reproducibility in signal linewidths. A strong correlation between 4T and 7T linewidths (Fig. 3) suggests that the small variation in the signal linewidth was

determined by intersubject variation in the properties of the selected brain tissue. The increase in spectral linewidth by 50% at 7T relative to 4T, corresponding to a 14% increase in spectral resolution of singlet resonances, is in very good agreement with published results (8).

Sensitivity profiles of half-volume RF coils are always nonuniform, which has to be taken into consideration when the gains in SNR between 4T and 7T are evaluated. An approximately two-fold increase in SNR, using the height of the NAA signal, was observed at 7T relative to 4T, which appeared to be in agreement with the theoretical prediction of the linear increase in SNR with B_0 (22). However, theoretical analysis predicts a linear increase in SNR for a constant linewidth, which did not hold for the 4T and 7T data. Taking into account the 1.5-fold increase in signal linewidth at 7T, the gain in corrected SNR between 4T and 7T was approximately three-fold, which corresponded to the gain in the integral-to-noise ratio calculated from the water reference spectra at 4T and 7T. To trace the source of the gain in SNR, the absolute values of signal intensities and noise levels were compared between 4T and 7T. The direct comparison can be questionable due to multiple modules in transmit and receive chains, the performances of which have a direct effect on observed values of signal and noise. Surprisingly, the observed gain in signal intensity (integrals) at 7T relative to 4T was proportional to B_0^2, as predicted from theory (22). However, absolute values of the observed noise intensities (root-mean-square deviations) did not increase linearly with the field as expected (22). This discrepancy could be explained by a smaller volume of the sample inducing the noise in 7T RF coil (23) resulting from slightly different shapes of the RF coil loops (elliptical vs. circular) and more limited penetration of the B_1^- field into the sample (see Figs. 1 and 8) (23,24). Consequently the expected increase of noise at 7T (22) was probably cancelled by a reduced volume of the sample interacting with the coil. A supralinear increase in SNR with field is in agreement with the results of other works (23,25,26). However, this observed gain in SNR between 4T and 7T is valid only for a specific location of the VOI inside the brain; i.e., for a specific location within the sensitive volume of the RF coils. Selecting the VOI deeper in the brain and further away from the RF coil would result in much less favorable gain in SNR at 7T relative to 4T because of the difference in sensitivity profiles of the RF coils used at 4T and 7T. These differences originate from increased nonuniformity of B_1^+ and B_1^- field distributions at higher frequencies when wavelengths become comparable with the size of the measured object (23-25).

Spectra acquired at two different field strengths were processed and quantified identically. LCModel basis sets for 4T and 7T were generated from the same NMR database of metabolite chemical shifts and J coupling constants. Acquiring data with a long repetition time (TR = 5 s) and ultrashort echo times (TE = 4–6 s) minimized the dependence of signal intensities on T_1 and T_2 relaxation processes; therefore, intensity corrections for "absolute" metabolite quantification were not necessary. Neurochemical profiles calculated from 4T and 7T ^{1}H NMR spectra were nearly identical (Fig. 4). In addition, data from individual subjects shown in scatter plots (Fig. 5) lay very close to the line of identity and exhibited a strong correlation, which suggests that the precision of metabolite quantification both at 4T and 7T was higher than the intersubject variation in metabolite levels. This implies that ultrahigh-field ^{1}H NMR spectroscopy is sensitive enough to detect subtle changes in metabolite concentrations between healthy subjects; therefore, substantially increased sensitivity to detect changes between healthy controls and patients with metabolic brain disorders is expected.

Metabolite quantification at 7T is less sensitive to decreasing SNR than the quantification at 4T (Fig. 6). All 17 metabolites could be quantified with reasonable accuracy from 7T spectra after four scans acquired from an 8-ml VOI. At 4T, reduced SNR resulted in systematic errors and the loss of sensitivity to detect several weakly represented metabolites. Only the quantification of Glc was better at 4T than at 7T. The highly J-coupled spin system of α- and

β-Glc is spread between 3.2 and 4.0 ppm under strong signals of other metabolites, such as Glu and *myo*-Ins. At 4T, some Glc multiplets collapse into a single peak, which makes the quantification of Glc easier at 4T, when the signal of H-1 of α-Glc at 5.22 ppm is not included in the LCModel analysis. Inclusion of the α-Glc signal in the fitting range for LCModel is expected to increase the reliability of glucose quantification at 7T; however, this requires the complete elimination of the residual water signal with postprocessing methods.

Increased SNR at 7T was not the only source for an increased precision of metabolite quantification (Figs. 6, 7, and 10). Increased chemical shift dispersion at 7T significantly reduced the CRLBs of all 17 quantified metabolites (Fig. 7), decreased the systematic errors in assessed metabolite concentrations introduced by low SNR (Fig. 6), increased the detectability of weakly represented metabolites, such as Asc, Asp, GABA, and PE at low SNR (Fig. 6), and increased the reliability to distinguish Gln from Glu and NAA from NAAG (Fig. 10). Decreased CRLBs at 7T relative to 4T are in agreement with the observed decrease in CRLBs at 4T relative to 1.5T (4) and 3T (9). Increased chemical shift dispersion at 7T especially improves the spectral resolution of J-coupled spin systems, such as Gln and Glu (12). The spectra of structurally similar molecules become more different from each other, which enables reliable quantification despite low SNR (Figs. 8 and 9). In other words, spectra in the LCModel basis set are more orthogonal at high magnetic fields, which means that any spectrum in the basis set cannot be substituted by a linear combination of other spectra from the same basis set. Consequently, the observed improvement in precision in metabolite quantification (decrease in CRLB) was approximately proportional to B_0^2. This noticeable improvement in detectability of metabolites was confirmed experimentally by comparing metabolite quantification from spectra acquired from 10 subjects at 4T with NT = 128 and at 7T with NT = 8 (Figs. 8 and 9).

Estimated correlation coefficients, derived from a standard least-squares variance-covariance matrix of LCModel analysis, indicated a strong negative correlation between Cr and PCr at both fields without any improvement at high SNR (Fig. 10a). This implies that the calculated concentration of Cr might be incorrectly increased at the expense of decreased PCr and vice-versa. Such a correlation would result in spreading of data points in a (PCr) vs. (Cr) plot along a line with a slope of −1. However, there is no indication that concentrations of PCr and Cr, quantified in 10 subjects, follow this line (Fig. 10d and g). The strong negative correlation between Cr and PCr estimated by LC-Model is the consequence of the insufficient separation between methylene signals of Cr and PCr relative to their linewidths. Difference in chemical shifts of 0.017 ppm corresponded to the difference of 2.9 Hz at 4T and 5.1 Hz at 7T, which was smaller than their linewidths (5.9 Hz at 4T and 9.8 Hz at 7T). Despite this estimated correlation, discrimination between Cr and PCr and their reliable quantification was possible (Figs. 4, 6, and 10). PCr concentrations determined both at 4T and 7T were in very good agreement with previously published values (27). The concentration ratio [PCr]/[Cr] ≈ 1 was consistently assessed from spectra with different SNR (Fig. 6) and is in agreement with values observed in the rodent brain under normal physiology (2,28,29). The higher precision in Cr and PCr quantification achievable at 7T was especially pronounced for spectra with low SNR (Fig. 7). However, the quantification of Cr and PCr is highly sensitive to spectral quality and data processing. Baseline distortions, poor water suppression, and even minor inaccuracies in chemical shifts of Cr and PCr in LCModel basis set may result in substantial systematic errors in Cr and PCr quantification.

In conclusion, this study clearly demonstrates advantages for in vivo ^{1}H NMR spectroscopy of the human brain at ultrahigh magnetic fields. Increased detection sensitivity for a broad range of brain metabolites implies that the total measurement time can be significantly reduced or the spatial resolution significantly increased at 7T relative to 4T without compromising the information content. These data indicate a great potential of in vivo ^{1}H NMR spectroscopy at

7T to reveal new information about the neuro-chemistry of human brain under normal and pathological conditions.

Acknowledgments

REFERENCES

1. Gruetter R, Weisdorf SA, Rajanayagan V, Terpstra M, Merkle H, Truwit CL, Garwood M, Nyberg SL, Ugurbil K. Resolution improvements in in vivo ^{1}H NMR spectra with increased magnetic field strength. J Magn Reson 1998;135:260–264. [PubMed: 9799704]

2. Pfeuffer J, Tkáč I, Provencher SW, Gruetter R. Toward an in vivo neurochemical profile: quantification of 18 metabolites in short-echo-time ^{1}H NMR spectra of the rat brain. J Magn Reson 1999;141:104–120. [PubMed: 10527748]

3. Barker PB, Hearshen DO, Boska MD. Single-voxel proton MRS of the human brain at 1.5T and 3.0T. Magn Reson Med 2001;45:765–769. [PubMed: 11323802]

4. Bartha R, Drost DJ, Menon RS, Williamson PC. Comparison of the quantification precision of human short echo time ^{1}H spectroscopy at 1.5 and 4.0 Tesla. Magn Reson Med 2000;44:185–192. [PubMed: 10918316]

5. Gonen O, Gruber S, Li BS, Mlynarik V, Moser E. Multivoxel 3D proton spectroscopy in the brain at 1.5 versus 3.0 T: signal-to-noise ratio and resolution comparison. AJNR Am J Neuroradiol 2001;22:1727–1731. [PubMed: 11673168]

6. Inglese M, Spindler M, Babb JS, Sunenshine P, Law M, Gonen O. Field, coil, and echo-time influence on sensitivity and reproducibility of brain proton MR spectroscopy. AJNR Am J Neuroradiol 2006;27:684–688. [PubMed: 16552016]

7. Kantarci K, Reynolds G, Petersen RC, Boeve BF, Knopman DS, Edland SD, Smith GE, Ivnik RJ, Tangalos EG, Jack CR Jr. Proton MR spectroscopy in mild cognitive impairment and Alzheimer disease: comparison of 1.5 and 3 T. AJNR Am J Neuroradiol 2003;24:843–849. [PubMed: 12748083]

8. Otazo R, Mueller B, Ugurbil K, Wald L, Posse S. Signal-to-noise ratio and spectral linewidth improvements between 1.5 and 7 Tesla in proton echo-planar spectroscopic imaging. Magn Reson Med 2006;56:1200–1210. [PubMed: 17094090]

9. Posse S, Otazo R, Caprihan A, Bustillo J, Chen H, Henry PG, Marjanska M, Gasparovic C, Zuo C, Magnotta V, Mueller B, Mullins P, Renshaw P, Ugurbil K, Lim KO, Alger JR. Proton echo-planar spectroscopic imaging of J-coupled resonances in human brain at 3 and 4 Tesla. Magn Reson Med 2007;58:236–244. [PubMed: 17610279]

10. Srinivasan R, Vigneron D, Sailasuta N, Hurd R, Nelson S. A comparative study of myo-inositol quantification using LCmodel at 1.5 T and 3.0 T with 3 D ^{1}H proton spectroscopic imaging of the human brain. Magn Reson Imaging 2004;22:523–528. [PubMed: 15120172]

11. Dydak U, Schär M. MR spectroscopy and spectroscopic imaging: comparing 3.0 T versus 1.5 T. Neuroimaging Clin North Am 2006;16:269–283.

12. Tkáč I, Andersen P, Adriany G, Merkle H, Ugurbil K, Gruetter R. In vivo ^{1}H NMR spectroscopy of the human brain at 7 T. Magn Reson Med 2001;46:451–456. [PubMed: 11550235]

13. Adriany G, Gruetter R. A half-volume coil for efficient proton decoupling in humans at 4 Tesla. J Magn Reson 1997;125:178–184. [PubMed: 9245377]

14. Gruetter R. Automatic, localized in vivo adjustment of all first- and second-order shim coils. Magn Reson Med 1993;29:804–811. [PubMed: 8350724]

15. Gruetter R, Tkáč I. Field mapping without reference scan using asymmetric echo-planar techniques. Magn Reson Med 2000;43:319–323. [PubMed: 10680699]

16. Tkáč I, Gruetter R. Methodology of ^{1}H NMR spectroscopy of the human brain at very high magnetic fields. Appl Magn Reson 2005;29:139–157. [PubMed: 20179773]

17. Tkáč I, Starčuk Z, Choi IY, Gruetter R. In vivo ^{1}H NMR spectroscopy of rat brain at 1 ms echo time. Magn Reson Med 1999;41:649–656. [PubMed: 10332839]

18. Provencher SW. Automatic quantitation of localized in vivo ^{1}H spectra with LCModel. NMR Biomed 2001;14:260–264. [PubMed: 11410943]

19. Provencher SW. Estimation of metabolite concentrations from localized in vivo proton NMR spectra. Magn Reson Med 1993;30:672–679. [PubMed: 8139448]

20. Govindaraju V, Young K, Maudsley AA. Proton NMR chemical shifts and coupling constants for brain metabolites. NMR Biomed 2000;13:129–153. [PubMed: 10861994]

21. Tkáč, I. Refinement of simulated basis set for LCModel analysis; Proceedings of the 16th Annual Meeting of ISMRM; Toronto, Ontario, Canada. 2008; Abstract 1624

22. Hoult DI, Lauterbur PC. Sensitivity of the zeugmatographic experiment involving human samples. J Magn Reson 1979;34:425–433.

23. Ocali O, Atalar E. Ultimate intrinsic signal-to-noise ratio in MRI. Magn Reson Med 1998;39:462–473. [PubMed: 9498603]

24. Wang J, Yang QX, Zhang X, Collins CM, Smith MB, Zhu XH, Adriany G, Ugurbil K, Chen W. Polarization of the RF field in a human head at high field: a study with a quadrature surface coil at 7.0 T. Magn Reson Med 2002;48:362–369. [PubMed: 12210945]

25. Keltner JR, Carlson JW, Roos MS, Wong ST, Wong TL, Budinger TF. Electromagnetic fields of surface coil in vivo NMR at high frequencies. Magn Reson Med 1991;22:467–480. [PubMed: 1812380]

26. Vaughan JT, Garwood M, Collins CM, Liu W, DelaBarre L, Adriany G, Andersen P, Merkle H, Goebel R, Smith MB, Ugurbil K. 7T vs. 4T: RF power, homogeneity, and signal-to-noise comparison in head images. Magn Reson Med 2001;46:24–30. [PubMed: 11443707]

27. Hetherington HP, Spencer DD, Vaughan JT, Pan JW. Quantitative ^{31}P spectroscopic imaging of human brain at 4 Tesla: assessment of gray and white matter differences of phosphocreatine and ATP. Magn Reson Med 2001;45:46–52. [PubMed: 11146485]

28. Tkáč I, Henry PG, Andersen P, Keene CD, Low WC, Gruetter R. Highly resolved in vivo ^{1}H NMR spectroscopy of the mouse brain at 9.4 T. Magn Reson Med 2004;52:478–484. [PubMed: 15334565]

29. Tkáč I, Rao R, Georgieff MK, Gruetter R. Developmental and regional changes in the neurochemical profile of the rat brain determined by in vivo ^{1}H NMR spectroscopy. Magn Reson Med 2003;50:24–32. [PubMed: 12815675]
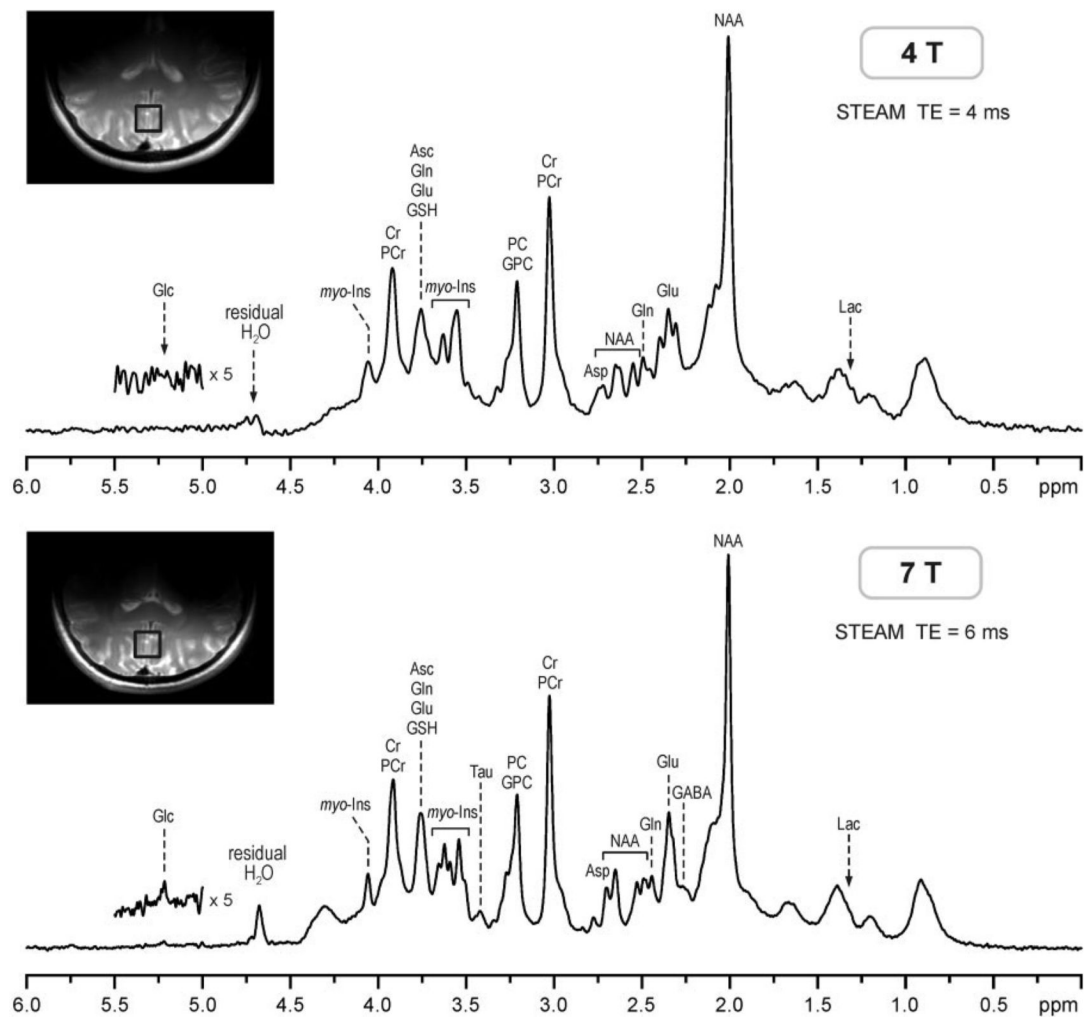
FIG. 1.
^{1}H NMR spectra acquired at 4T and 7T from the brain of the same subject. STEAM, TE = 4 ms (4T), TE = 6 ms (7T), TR = 5 s, VOI = 8cm³, NT = 160. Processing: frequency and phase correction of single-scan FID arrays, FID summation, correction for the residual eddy currents, Gaussian multiplication (σ = 0.15 s), FT, zero-order phase correction. SNR = 149 (4T), SNR = 303 (7T). Insets: transverse RARE images of the brain with the position of the VOI on the midline in the occipital lobe.
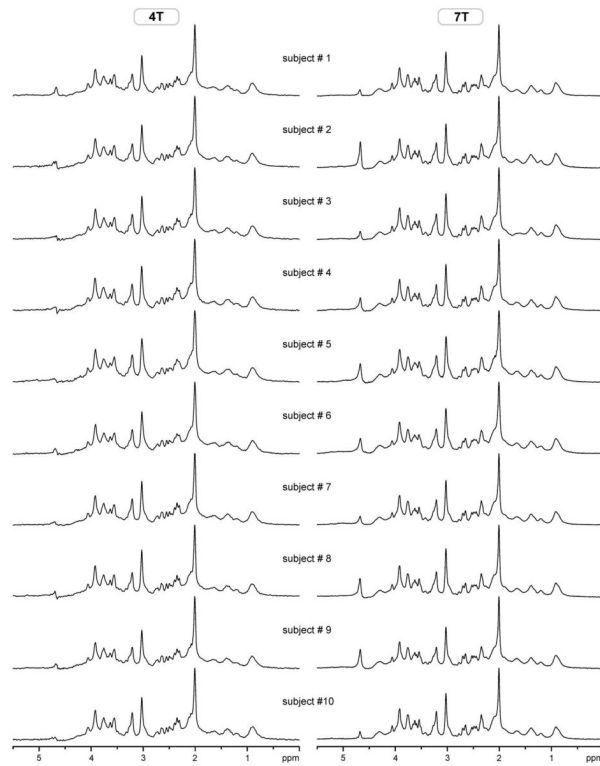
FIG. 2.
In vivo ^{1}H NMR spectra of 10 healthy subjects measured at 4T and 7T. Data acquisition and processing parameters were the same as in Fig. 1. No water signal removal or baseline corrections were applied. Average SNR = 154 (4T), SNR = 307 (7T).
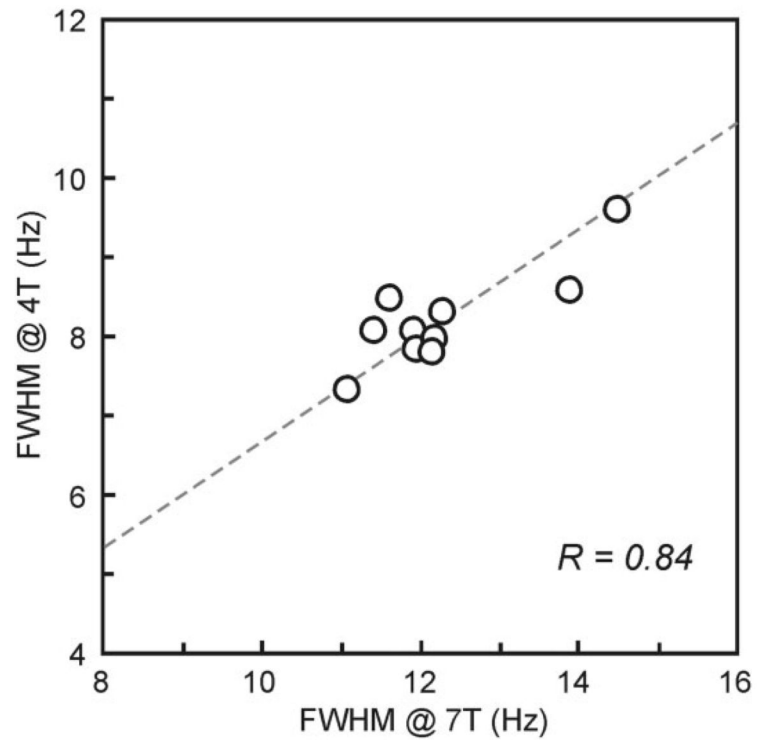
FIG. 3.
Correlation between water signal linewidths of individual subjects achieved at 4T and 7T. Gray matter–rich occipital cortex, VOI = 8 cm^3, see Fig. 1 for the location.
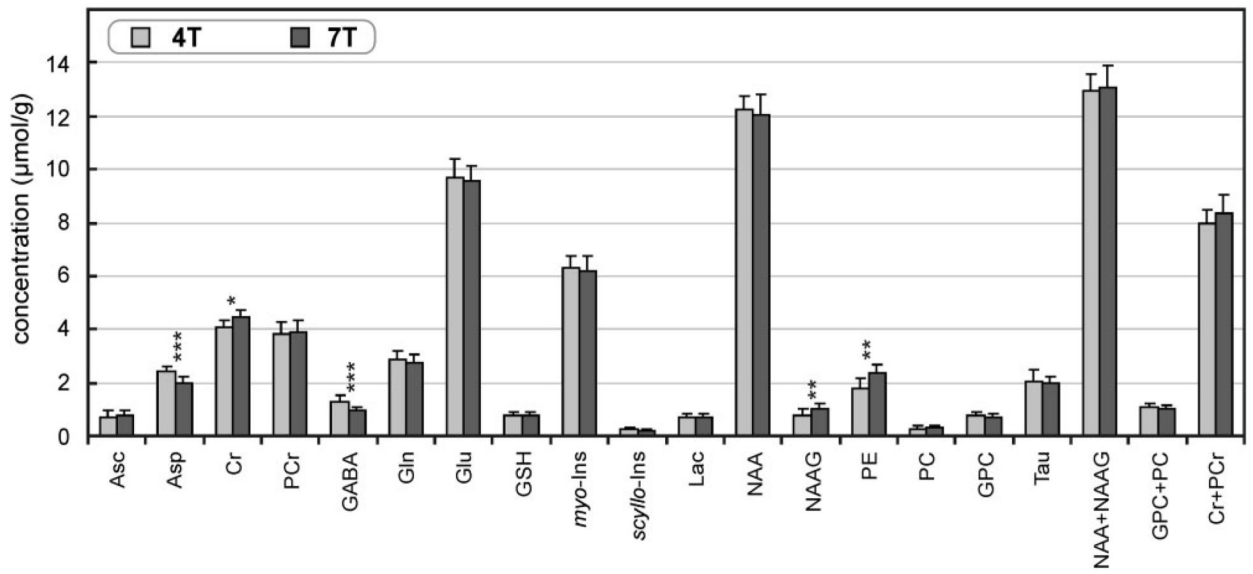
FIG. 4.
Comparison of neuro-chemical profiles determined at 4T and 7T from gray-matter–rich occipital cortex of 10 healthy volunteers (age = 24 ± 5 years). ^{1}H NMR spectra with NT = 160, error bars = SD, significance level: *$P < 0.05$, **$P < 0.01$, ***$P < 0.001$.
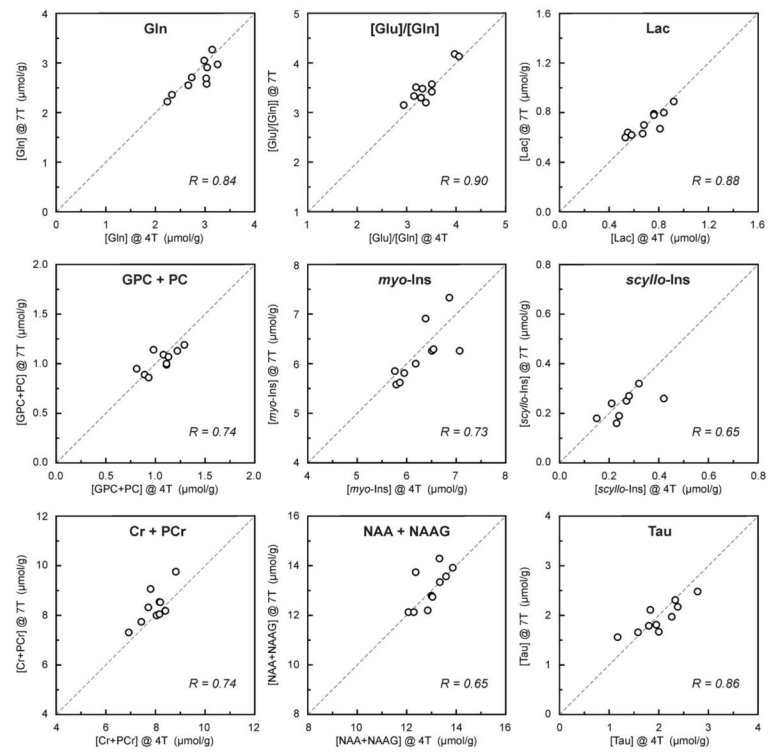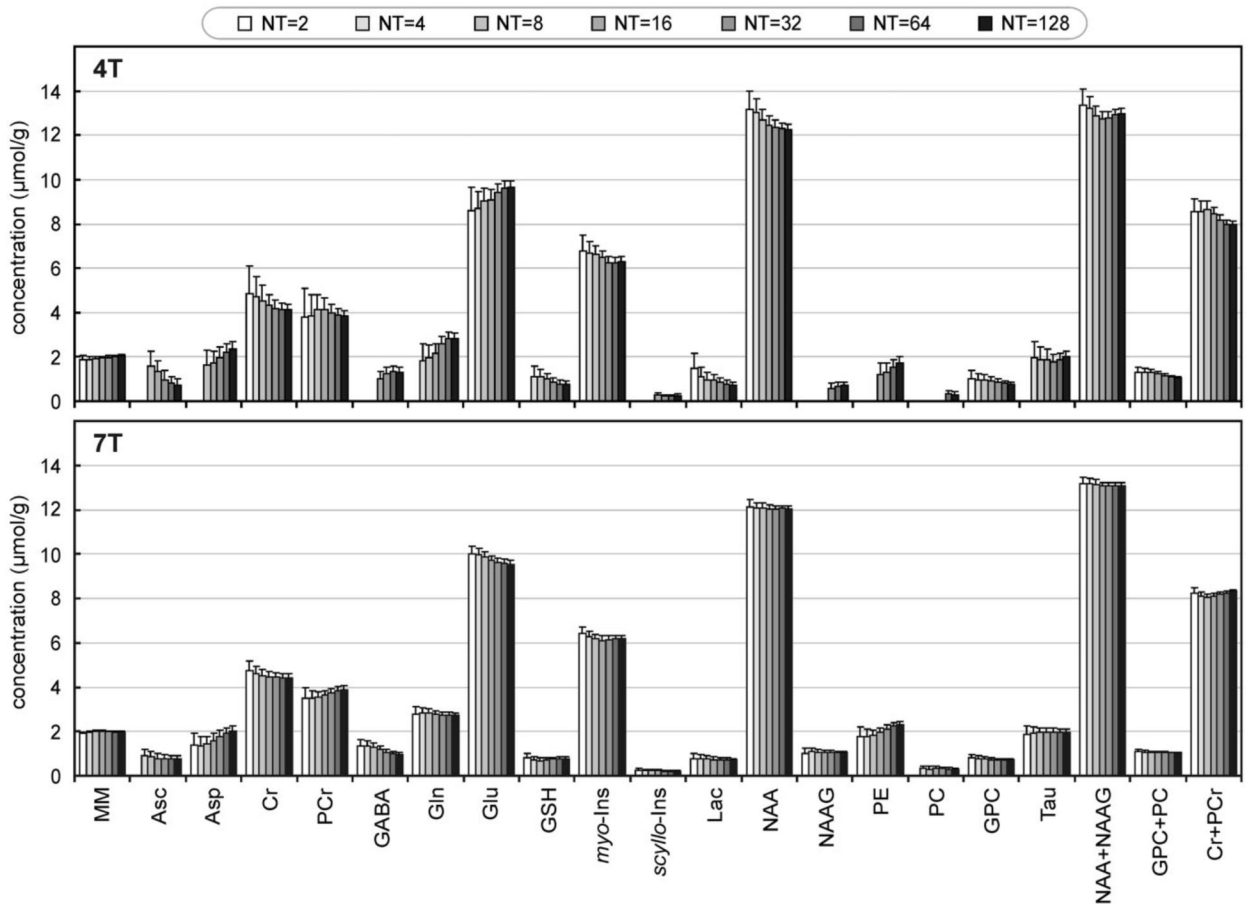
FIG. 5.
Correlation between metabolite concentrations of individual subjects determined from 4T and 7T spectra (NT = 160).

FIG. 6.
Metabolite concentrations determined at 4T and 7T from spectra with number of transients ranging from 2 to 128. Number of subjects = 10, number of spectra per subject: 10 spectra with NT = 2, 10 × NT = 4, 10 × NT = 8, 10 × NT = 16, 5 × NT = 32, 2 × NT = 64, 1 × NT = 128. Error bars: average Cramér-Rao lower bounds. Metabolites such as GABA, *scyllo*-Ins, NAAG, and PC were not detected from spectra with lower number of transients at 4T (CRLB > 50%). Macromolecules (MM) are quantified in arbitrary units.
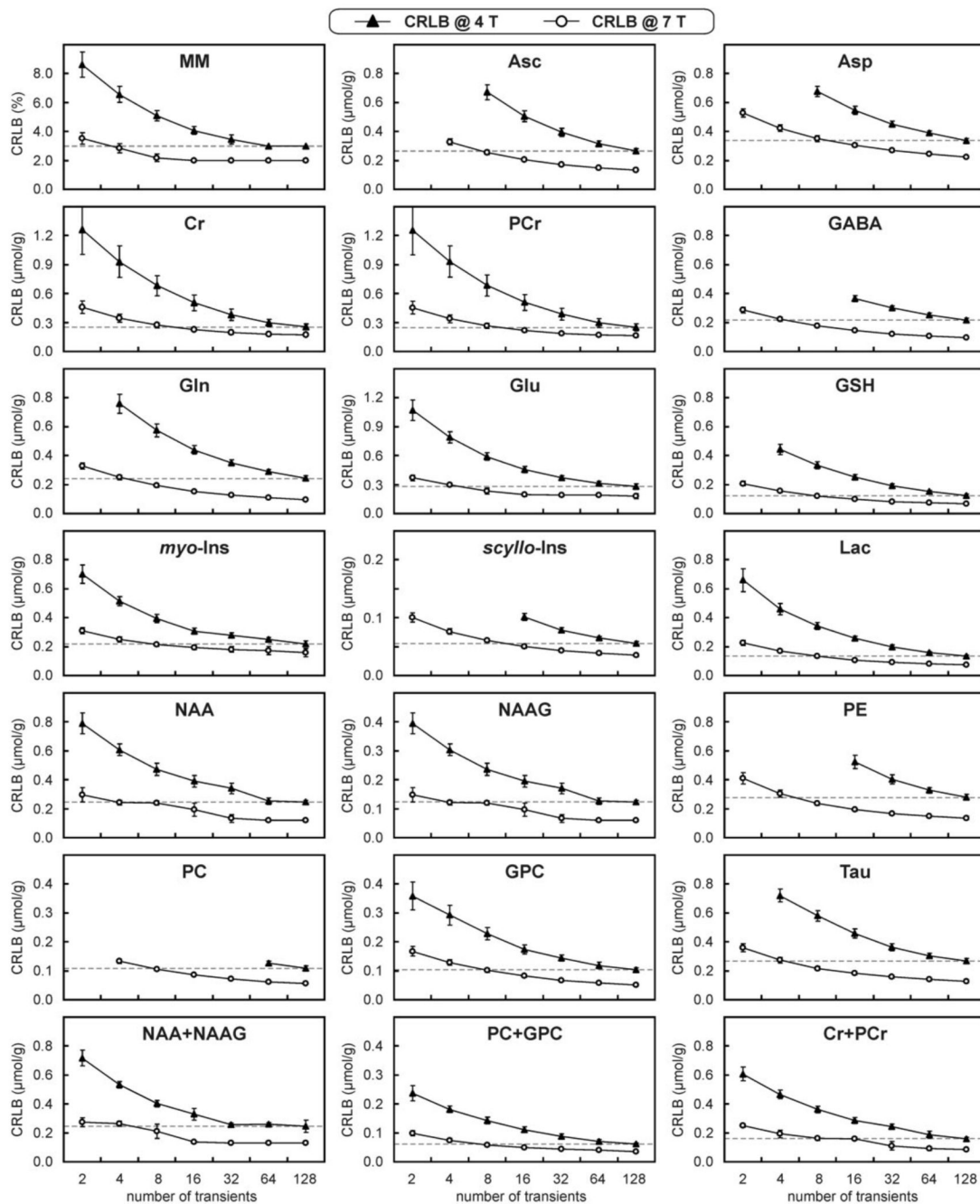
FIG. 7.
Comparison of Cramér-Rao lower bounds (CRLBs) of brain metabolites and fast-relaxing macromolecules (MM) between 4T and 7T as a function of the number of transients. Number of subjects and number of spectra per subject are the same as in Fig. 6. Error bars = SD. Horizontal lines represent the CRLB achieved with NT = 128 at 4T.
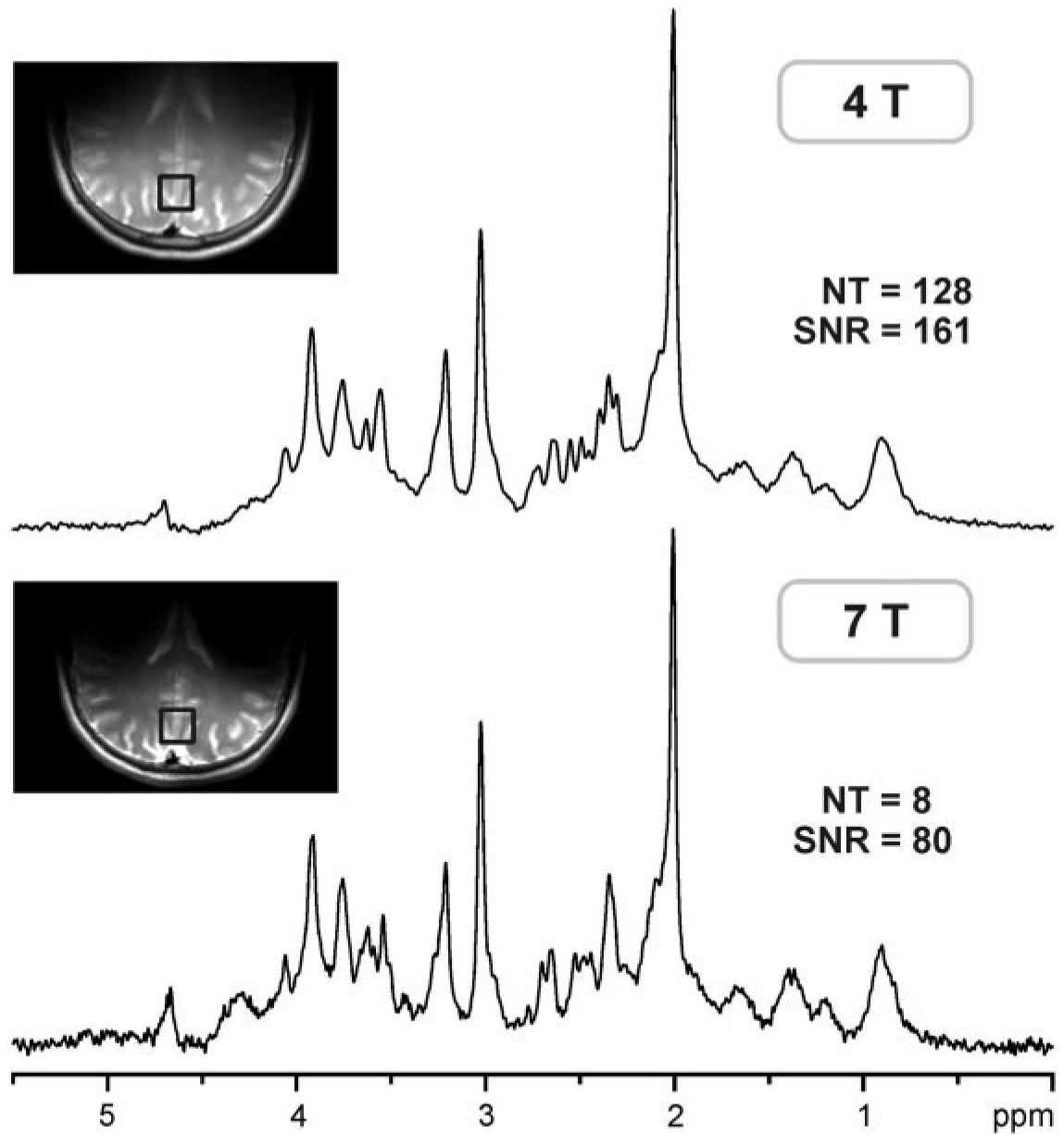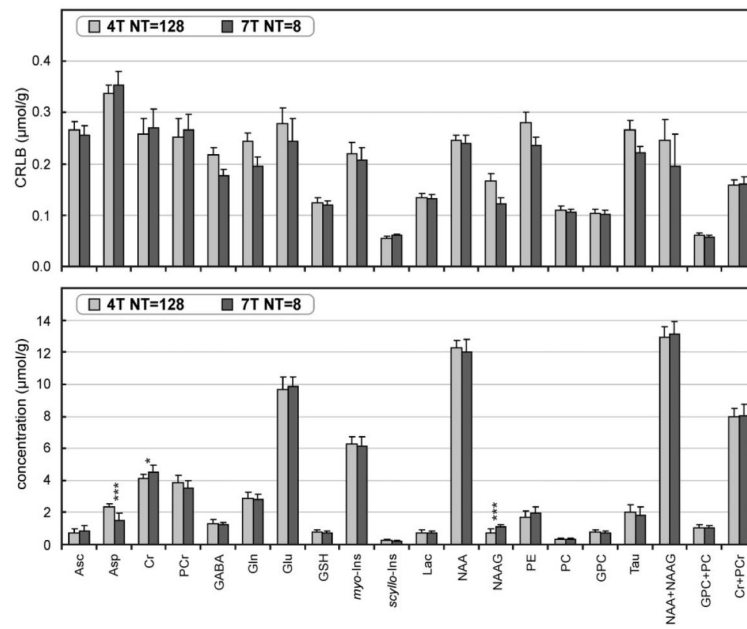
FIG. 8.
Representative ^{1}H NMR spectra of one subject measured at 4T with 128 transients and at 7T with eight transients. Insets: transverse RARE images of the brain with the position of the VOI on the midline in the occipital lobe.

FIG. 9.
Concentrations of brain metabolites and corresponding CramérRao lower bounds quantified by LC-Model analysis from spectra measured at 4T with 128 transients and at 7T with eight transients. Number of subjects = 10, number of spectra per subject and field strength = 1, error bars = SD, significance level: *$P < 0.05$, ***$P < 0.001$.
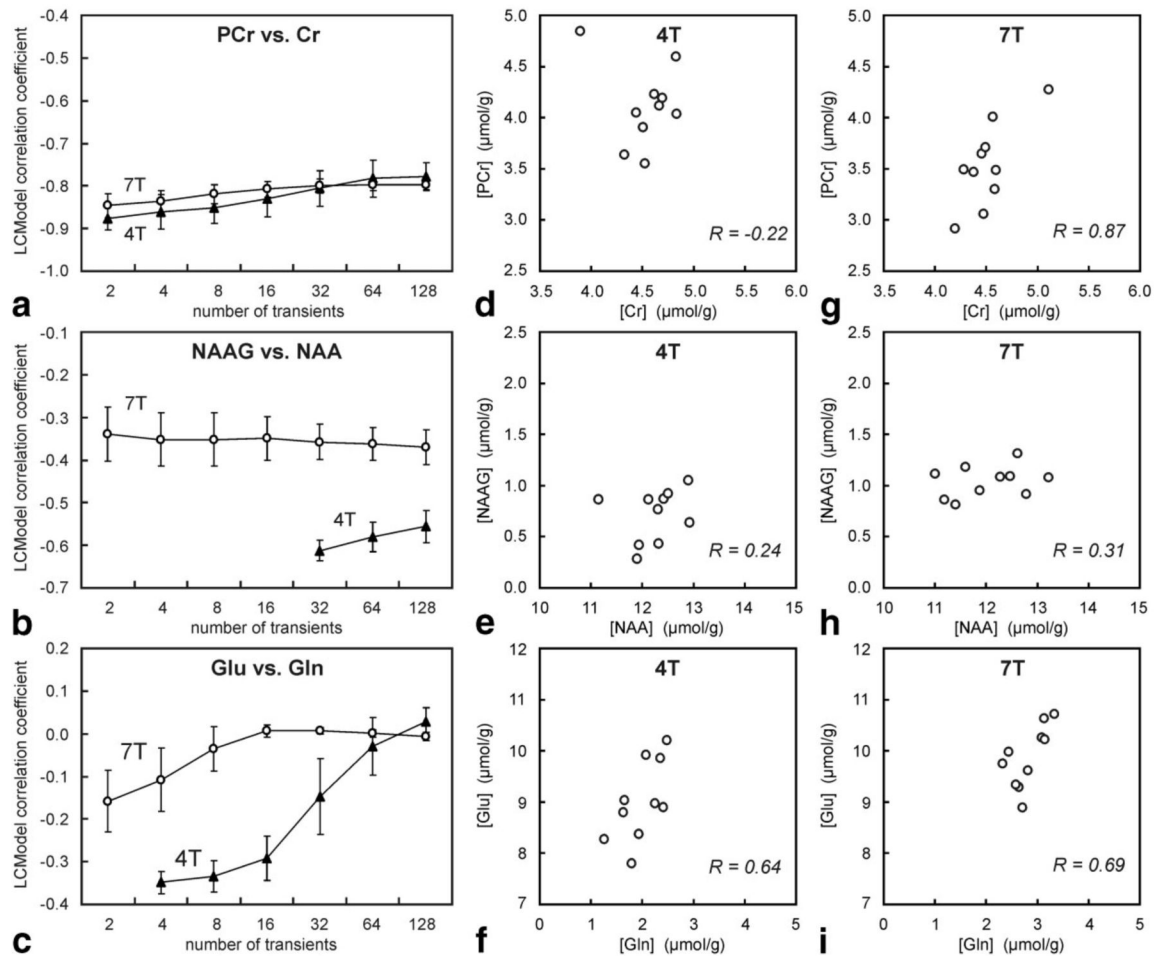
FIG. 10.
Comparison of correlation coefficients of selected pairs of metabolites estimated by LCModel analysis of 4T and 7T spectra (**a**–**c**) with the correlation between the concentrations of these metabolites measured in 10 subjects at 4T (**d**–**f**) and 7T (**g**–**i**). LCModel correlation coefficients are presented as a function of a number of transients (a-c). Scatter plots (d,g) PCr vs. Cr (NT = 8); (e,h) NAAG vs. NAA (NT = 128); (f,i) Glu vs. Gln (NT = 8) document that strong negative correlations between these pairs of metabolites were not observed. Number of subjects and number of spectra per subject are the same as in Fig. 6.